

Thermal stability of bidentate nitrogen ligands tethered to multiwall carbon nanotubes

Bob A. Howell · Adina Dumitrascu

NATAS2009 Special Issue
© Akadémiai Kiadó, Budapest, Hungary 2010

Abstract Bidentate nitrogen ligands, particularly 1,10-phenanthroline, form stable complexes with a variety of divalent metal ions. If these ligands are attached to a stable, inert platform, then they may be used for sequestering transition metal ions from a range of aqueous solutions including many that form components of industrial processes. Alternatively, they may function as a base for the development of durable heterogeneous catalysts. These ligands may be tethered to carboxyl-functionalized carbon nanotubes via an ethylene oxide linker through either an ether or ester bond. The suitability of these adducts for a variety of applications has been assessed using thermogravimetry. Both kinds of adducts are thermally robust with an onset of degradation above 400 °C.

Keywords Carbon nanotube functionalization · Immobilized chelating ligands · Durable heterogeneous catalysts · Water treatment

Introduction

Since their discovery nearly two decades ago, carbon nanotubes have inspired much work directed toward an understanding of their properties and potential application in a wide range of fields [1–5]. Carbon nanotubes are produced commercially by several techniques [6, 7]. These often contain significant levels of impurities, principally metal catalyst residues and amorphous carbon. Impurities

may be removed, to a greater or lesser degree, by treatment with acid. Carbon nanotubes are strongly hydrophobic, tend to associate in bundles, and, in an unmodified state, incompatible with many matrices. For most applications, the nanotube surface must be modified. While physical methods of surface modification have been widely explored, covalent alteration of the surface has been most useful. Although many methods have been used, this is most generally accomplished by treatment of the nanotubes with a 3:1 mixture of concentrated aqueous sulfuric and nitric acids [8, 9]. This treatment promotes intercalation/exfoliation of the tubes, removes impurities, cuts the tubes (particularly, when acid treatment is used in conjunction with sonication), and effects oxidation at structural defects, principally tube ends, to introduce oxygen-containing functionality, primarily carboxyl groups, at the tube surface. The level of carboxylation achieved has been estimated by a number of methods including acid–base titration [10, 11], infrared spectroscopy [12], mass increase on salt formation upon reaction with dodecylamine [8], and various microscopy techniques [4]. The presence of carboxyl groups at the surface provides an anchor for the attachment of a variety of groups intended to make the nanotubes suitable for a particular application. For the generation of nanocomposites, groups are attached to make the nanotubes compatible with a polymer matrix [13]. In some instances, the polymer may be directly grafted to the nanotube [14, 15]. This may be done by either a “grafting to” or “grafting from” approach. The “grafting to” method often utilizes the ability of propagating species to add to the unsaturation of the carbon nanotubes [16–18]. In other cases, the preformed end-functionalized polymer is attached by esterification, amidation, or other coupling reaction [19, 20]. In general, the “grafting to” methods lead to low levels of grafted polymer and non-uniform

B. A. Howell (✉) · A. Dumitrascu
Center for Applications in Polymer Science, Department
of Chemistry, Central Michigan University, Mt. Pleasant,
MI 48859-0001, USA
e-mail: bob.a.howell@cmich.edu

distribution on the nanotube surface. The “grafting from” approach involves the immobilization of an initiator on the surface of the nanotubes followed by surface-initiated polymerization to grow polymer directly from the nanotube surface [21]. Many kinds of polymers may be attached and high graft density achieved. This approach is amenable to all the quasi-controlled radical polymerization techniques. Attachment of appropriate initiator molecules permits atom transfer radical polymerization (ATRP) [22–25], reversible addition fragmentation chain transfer (RAFT) [26, 27], and nitroxyl-mediated radical polymerization (NMRP) [28] from the nanotube surface. These methods allow the size of polymer layer at the surface of the nanotube to be controlled.

The utilization of surface-modified carbon nanotubes in biological applications, for example, as biosensors [29] and, more importantly, as drug delivery vehicles [30–35] has great potential. Functionalized, water-soluble carbon nanotubes are able to traverse the cell membrane by endocytosis to deliver a chemotherapeutic agent [33]. This has been wonderfully exploited for the delivery of organoplatinum prodrugs [34, 35]. Approximately 65 platinum(IV) units per nanotube may be loaded [35]. This is comparable to the number of (diaminocyclohexane)platinum(II) units that may be attached to the surface of a generation 4.5 poly(amidoamine) [PAMAM] dendrimer [36]. Further, the multi-valent nanotube prodrug may be functionalized with a folate component to specifically target folate receptor-enriched tumor cells [34].

Experimental

Materials

Multi-walled carbon nanotubes (MWCNTs) COOH functionalized (–COOH content: 2.56 wt%) of 10–50 μm length, 8–15 nm outside diameter, and 3–5 nm inside diameter were purchased from Cheap Tubes Inc. All other chemicals were purchased from Aldrich or Alfa Aesar and used as received without further purification. All organic solvents were dried and freshly distilled prior to use.

Methods and instrumentation

Thermogravimetric analyses (TG) were carried out using a TA Instruments model 2950 TGA unit interfaced with the 2100 control module. The TG cell was swept with nitrogen or air at 20 mL min^{-1} during degradation runs. The sample size was 5–10 mg in a platinum sample pan. Heating rate: 10 $^{\circ}\text{C min}^{-1}$, after equilibration at 40 $^{\circ}\text{C}$. Fourier transform infrared (FT-IR) spectra were obtained using solid solutions ($\sim 1\%$) in anhydrous potassium bromide (as pellets) using a

model 560 Nicolet MAGN-IR spectrophotometer. Nuclear magnetic resonance (NMR) spectra (^1H and ^{13}C) were obtained using solutions in DMSO- d_6 or CDCl_3 containing tetramethylsilane (TMS) as an internal reference and a Varian Plus 300 spectrometer. Direct insertion probe mass spectrometry (DIP-MS) was used to determine the molecular mass of the phenanthroline compounds. Bath sonication (Branson 3510) and filtration using polycarbonate membrane filters (Millipore) were employed for the reactions/separations of functionalized MWCNTs.

Synthesis

1,10-Phenanthroline-5,6-epoxide

To a mechanically-stirred aqueous solution of commercial hypochlorite (CLOROX) (1800 mL) maintained at 18 $^{\circ}\text{C}$, was added tetrabutylammonium hydrogensulfate (4.47 g, 0.0132 mol) and the pH of the resulting solution was adjusted to 8.2–8.3 by addition of aqueous concentrated hydrochloric acid solution. To this, a solution of 1,10-phenanthroline monohydrate (6 g, 0.033 mol) in dichloromethane (600 mL) was added, and the pH of the reaction mixture was carefully maintained between 8.2 and 8.6 by addition of 50% aqueous sodium hydroxide solution. Progress of the reaction was followed by NMR and TLC (Whatman silica gel-coated plates 60 F₂₅₄ and AcOEt-*i*PrOH-conc. NH_3 aq. = 8:4:1 as a developing system) because the reaction time varies as a function of the pH of the reaction mixture and of quality of the hypochlorite solution. Also, the yield decreases over time. After the reaction was complete, the layers were separated and the organic layer washed with a large excess of cold water. The solution was dried over anhydrous magnesium sulfate, and the solvent was removed by rotary evaporation at reduced pressure. The residual solid was stirred as a suspension in a 1:3 chloroform-acetone mixture. The solid was collected by filtration at reduced pressure to provide 5.5 g (93.2% yield) of 1,10-phenanthroline-5,6-epoxide as a yellow powder, m.p. 160–162 $^{\circ}\text{C}$: $^1\text{H-NMR}$ (300 MHz, CDCl_3): δ 4.6 ppm (2H, s, phenH-5&6), 7.36–7.4 ppm (2H, dd 7.6, 4.6 Hz, phenH-8 + 3), 7.97–8.0 ppm (2H, dd 7.6, 1.7 Hz, phenH-4 + 7), 8.89–8.91 ppm (2H, dd, 4.6, 1.7, phenH9&2); $^{13}\text{C-NMR}$ (75.46 MHz, CDCl_3): δ 150.39 ($\text{C}_2 + \text{C}_9$), 149.03 ($\text{C}_{10a} + \text{C}_{10b}$), 137.95 ($\text{C}_4 + \text{C}_7$), 128.78 ($\text{C}_{4a} + \text{C}_{6a}$), 123.423 ($\text{C}_8 + \text{C}_3$), 54.83 ($\text{C}_5 + \text{C}_6$); IR (KBr): 3003, 1579, 1560, 1475, 1431, 1216, 1189, 1131, 1080, 1012, 883, 799, 750, 705 cm^{-1} [37–41].

5-Hydroxy-1,10-phenanthroline monohydrate

5,6-Epoxy-1,10-phenanthroline (310 mg, 1.58 mmol) was gradually added over about 20 min to a stirred and ice-water

cooled sample of concentrated aqueous sulfuric acid solution (10 mL). The initially bright yellow solution was heated to 100 °C for 1.0 h. The color of the mixture changed to dark brown during heating. The mixture was allowed to cool to room temperature and was slowly diluted with cold distilled water (about 50 mL). The diluted acid solution was neutralized to pH = 7 by slowly adding 50% aqueous sodium hydroxide solution. During the neutralization, the temperature was kept strictly between 0 and 5 °C, using a salt-ice bath and by adding ice into the solution. A black insoluble residue formed if the temperature was not maintained below 5 °C during neutralization. At pH = 7, a very fine maroon powdery precipitate formed. Centrifugation of the suspension pelletized the powder, and the supernatant was decanted. The powder was re-suspended in water (50 mL) and pelletized again with centrifugation. This operation was repeated and the resulting precipitate was dried in an Abderhalden drying unit at reduced pressure, over phosphorous pentoxide, for 3 days, to obtain 300 mg (88.75%) of 5-hydroxy-1,10-phenanthroline as a dark red solid, m.p. 210–211 °C: ¹H-NMR (300 MHz, DMSO-d₆): δ 10.9 (broad, s, 1H, OH), 9.09 (1H, d, phenH-2), 8.8 (1H, d *J* = 8.2 Hz, phenH-9), 8.6 (1H, d *J* = 7.8, phenH-4), 8.23 (1H, d, *J* = 8.2 Hz, phenH-7), 7.72–7.76 (1H, dd *J* = 8.2, 4.3 Hz, phenH-3), 7.57–7.61 (1H, dd *J* = 8.2, 4.3 Hz, phenH-8), 7.12 (1H, s, phen H-6), 3.4 (s, H₂O). ¹³C-NMR (75.46 MHz, CD₃OD): δ 150.85 (C₅), 150.07 (C₂), 146.6 (C_{10a}), 146.4 (C₉), 146.153(C_{10b}), 134.14 (C₄), 130.51 (C₇), 129.65 (C_{6a}), 123.31 (C₃), 123.19 (C₈), 122.77 (C_{4a}), 103.93 (C₆). IR (KBr): 3438, 2955, 1652, 1506, 1419, 1124, 1070, 1008, 832, 739, 703 cm⁻¹. DIP-MS: calcd. for C₁₂H₈N₂O 196, found 196. The solid is insoluble in usual organic solvents such as chloroform, methylene chloride, acetone, ethyl acetate, toluene, acetonitrile, DMF, THF, ether, but is slightly soluble in DMSO and methanol [40, 42, 43].

5-(2-Hydroxyethoxy)-1,10-phenanthroline

A solution of 5-hydroxy-1,10-phenanthroline monohydrate (428 mg, 2.00 mmol) and potassium carbonate (304 mg, 2.2 mmol) in 10 mL of DMF was stirred at 60 °C under nitrogen for 2 h. A clear orange solution was formed and allowed to cool to room temperature. Ethylene oxide was bubbled into the stirred solution for 20 min (at a rate of about 1 bubble per second). A slight exothermic effect was noticed, and the color of the solution changed to maroon. The mixture was then stirred at room temperature for three hours and a new portion of ethylene oxide was bubbled into the solution for 10 min (no changes in the appearance of the solution were noticed). The mixture was stirred overnight at room temperature, neutralized to pH = 7 with concentrated aqueous sulfuric acid solution, and the solvent distilled at reduced pressure. A dark red powder was

obtained: ¹H-NMR (300 MHz, DMSO-d₆) δ 8.95 (dd, *J* = 1.5, 4.2 Hz, 1H), 8.72–8.80 (m, 1H); 8.51 (m, 1H), 7.78–7.88 (m, 1H), 7.58–7.68 (m, 1H), 7.34 (dd, *J* = 4.2; 8.1, 1H), 6.72 (s, 1H), 4.28 (t, *J* = 4.4, 2H), 3.91 (t, *J* = 4.4, 2H); IR (KBr): 3406, 2935, 2627, 1653, 1506, 1419, 1301, 1259, 1218, 1124, 1071, 1008, 981, 831, 739, 703 cm⁻¹. The product is insoluble in almost all organic solvents and has a very modest solubility in DMSO and methanol. The DIP-MS spectrum contained a molecular ion peak at *m/z* 240, consistent with the attachment of a single ethylene oxide residue to the phenolic hydroxyl group [40, 44].

MWCNT-CH₂OH

To a stirred solution of 3.65 g MWCNT (2.56% carboxyl-functionalized; 0.093 g, 2.07 mmole of carboxyl functionality) in 100 mL of anhydrous THF was added, dropwise, over a period of 0.25 h, a solution of 1 M borane in THF (3.5 mL, 3.5 mmol). On completion of the addition, the mixture was allowed to stir overnight at room temperature. Water (10 mL) was added to remove excess borane and the suspended solid collected by filtration at reduced pressure. The solid was washed repeatedly with acetone and then dried at reduced pressure to provide MWCNT-CH₂OH [45, 46].

MWCNT-CH₂OTs

To a stirred suspension of 3.50 g MWCNT-CH₂OH and 1 mL (0.726 g, 7.18 mmole) of triethylamine in 100 mL of dry dichloromethane maintained in a nitrogen atmosphere was added, dropwise, over a period of 0.25 h, a solution of 0.43 g (2 mmol) of *p*-toluenesulfonyl chloride in 10 mL dichloromethane. The resulting mixture was stirred 16 h at room temperature. The nanotubes were collected by filtration at reduced pressure and washed, successively, with several portions of first dichloromethane and then methanol [47, 48].

MWCNT-Phen-ether

To a stirred solution of 5-(2-hydroxyethoxy)-1,10-phenanthroline (200 mg, 0.833 mmol) in 10 mL DMF maintained in a nitrogen atmosphere was added 36 mg (0.9 mmol; 60% suspension in mineral oil) of sodium hydride. Hydrogen evolution was noted. The solution was stirred for 0.5 h at room temperature. A suspension of 1.58 g MWCNT-CH₂OTs (0.9 mmol of tosylate functionality) was added and the resulting mixture was stirred 24 h at room temperature. The solid was collected by filtration at reduced pressure, washed with several portions of methanol and acetone, and dried at reduced pressure and room temperature.

MWCNT-COCl

A suspension of 500 mg MWCNT-COOH (2.56% carboxyl-functionalized; 12.8 mg, 0.28 mmole of carboxyl functionality) in 250 mL of thionyl chloride containing a few drops of *N,N*-dimethyldimethylformamide (DMF) was subjected to sonication for 0.5 h and then stirred at thionyl chloride reflux for 24 h. The MWCNT-COCl was collected by filtration at reduced pressure, washed with several portions of THF and dried at reduced pressure and room temperature.

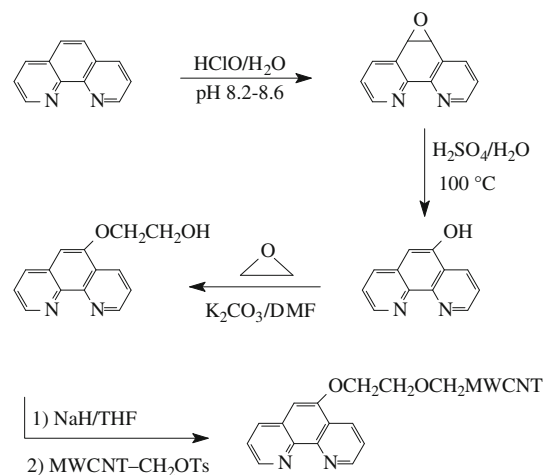
MWCNT-Phen-ester

To a cold (0 °C), stirred suspension of 200 mg MWCNT-COCl (7.22 mg, 0.11 mmole of acid chloride functionality) in 150 mL of DMF was added, portionwise, a solution of 200 mg (0.83 mmol) of 5-(2-hydroxyethoxy)-1,10-phenanthroline and 5.0 mL (4.9 g, 0.061 mol) of pyridine in 25 mL of DMF. The resulting mixture was maintained in a nitrogen atmosphere with constant stirring and intermittent sonication for 3 days. The solid was collected by filtration at reduced pressure, washed with several portions of methanol, and dried at reduced pressure and room temperature.

Results and discussion

1,10-Phenanthroline presents several attractive structural and chemical properties. Perhaps, the greatest of these is its remarkable chelating capability [49, 50]. 1,10-Phenanthroline forms stable complexes with a wide variety of metal cations including, importantly, those of the platinum group metals [37, 51]. Attachment of a phenanthroline moiety to a stable, relatively inert platform could form the base for a family of heterogeneous catalysts that would be readily separable from product mixtures and recyclable. In this instance, 1,10-phenanthroline has been anchored to MWCNTs via a tether. The most suitable route to an appropriate structure is shown in Scheme 1. 1,10-Phenanthroline was converted to the 5,6-epoxide by treatment of a dichloromethane solution with aqueous hypochlorite in the presence of a phase-transfer catalyst at pH 8.4 [37–41]. The pH of the aqueous phase must be maintained between 8.2–8.6. At higher pH, very little epoxidation occurs, and at lower pH, other oxidation products, principally 5,6-dichloro-5,6-dihydro-1,10-phenanthroline and 5-chloro-6-hydroxy-5,6-dihydro-1,10-phenanthroline, are formed.

Conversion of the epoxide to 5-hydroxy-1,10-phenanthroline could be accomplished by treating it with concentrated aqueous sulfuric acid [40, 42, 43]. This transformation



Scheme 1 Attachment of a 1,10-phenanthroline unit to MWCNT via an ethylenedioxy tether

is reflected in the proton NMR spectra contained in Fig. 1. The spectrum for the 5-hydroxy compound contains absorption at δ 7.12 for the proton at C-6 and at δ 10.9 for the hydroxyl proton. 5-Hydroxy-1,10-phenanthroline is insoluble in most organic solvents but is modestly soluble in dimethyl sulfoxide and methanol. It displays an onset temperature for degradation of 329 °C as determined by thermogravimetry.

5-Hydroxy-1,10-phenanthroline was converted to the corresponding 2-hydroxyethyl ether by treatment with ethylene oxide in dimethylformamide in the presence of potassium carbonate [40, 44]. Conversion of the alcohol to the alkoxide and treatment with MWCNT containing primary tosylate groups at the surface permitted coupling to the nanotubes. The tosylate-functionalized tubes were prepared by borane reduction of carboxyl-functionalized tubes followed by esterification with *p*-toluenesulfonyl chloride (Scheme 2) [45–48].

These transformations were most conveniently monitored by thermogravimetry and infrared spectroscopy. Figure 2 contains decomposition thermograms for functionalized nanotubes, carboxyl through the ether-linked phenanthroline ligand. The indicated transformations are clearly evident in these thermograms.

Consistent with earlier observations, nanotubes with more complex substitution display lower thermal stability than do the corresponding structures with simpler substituents [23, 24, 28]. It has been suggested that the presence of substituent fragments and a less perfect structure after modification make carbon nanotubes more susceptible to thermal degradation [23].

Carboxyl-functionalized MWCNTs are stable in nitrogen to well above 800 °C. Reduction of the carboxyl groups to methylol functionality brings about a significant reduction in stability with degradation onset half that of the

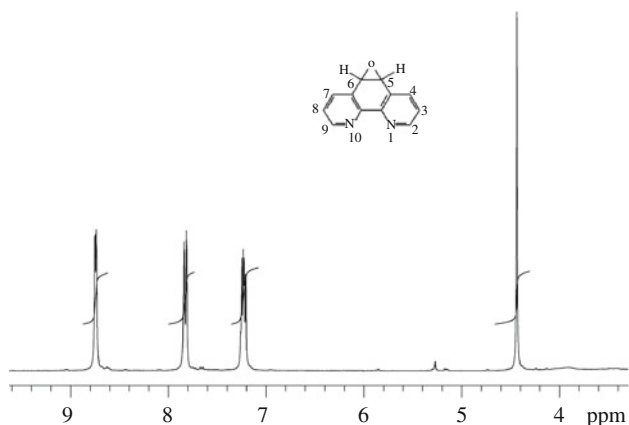
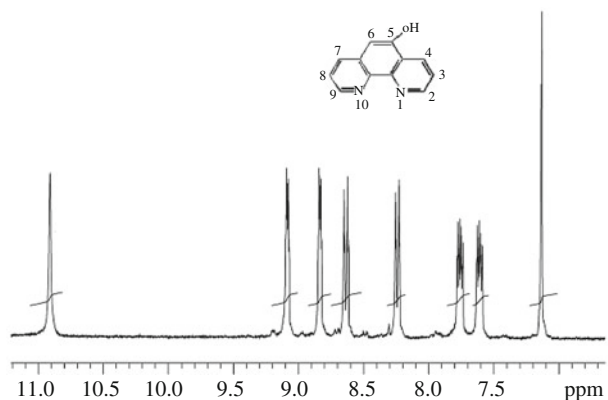
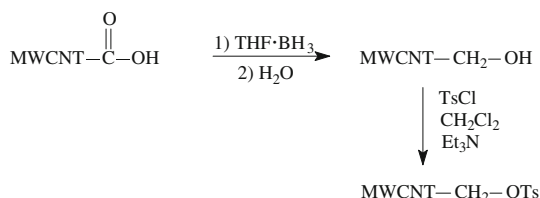


Fig. 1 Proton NMR spectra of 1,10-phenanthroline-5,6-epoxide and 5-hydroxy-1,10-phenanthroline



Scheme 2 Generation of tosylate-functionalized MWCNTs



simple carboxyl-functionalized material. Conversion of the alcohol groups to tosylate esters improves the stability only marginally. Displacement of the tosylate anion by ethoxylated ligand affords the ether-tethered product. This, too, undergoes smooth decomposition at a temperature comparable to those at which the alcohol or the ester degrades. This degradation is much smoother than that for the ethoxylated ligand itself, which may suggest that the principal degradative event for this and the other derivatives is cleavage from the MWCNT. As is clearly shown in Fig. 3, the ether-linked ligand undergoes smooth, single-step degradation with an extrapolated onset at 404 °C.

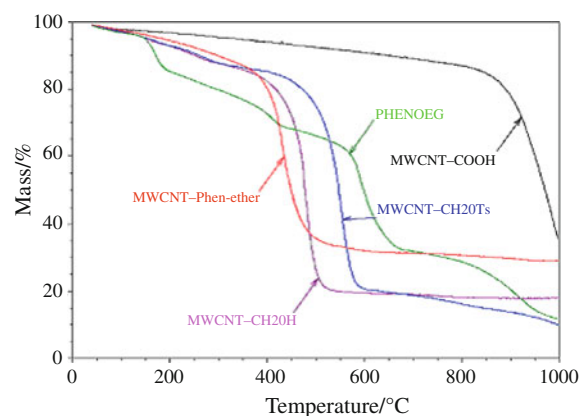


Fig. 2 Thermal degradation in a nitrogen atmosphere of functionalized MWCNT-carboxyl through ether-linked phenanthroline

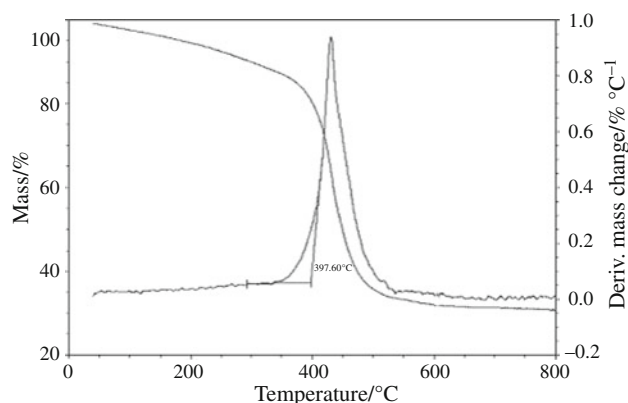


Fig. 3 Thermal degradation in a nitrogen atmosphere of MWCNT containing ether-linked phenanthroline at the surface

The infrared spectra of the various adducts are supportive of the structures indicated (see Fig. 4).

As noted on the spectra, expected changes occur as the carboxyl-functionalized MWCNT are converted to the corresponding phenanthroline-functionalized material. In the FTIR spectrum of oxidized MWCNT (A), the peak at $\sim 1720 \text{ cm}^{-1}$ may be attributed to the C=O stretch of the carboxylic (COOH) group and the peak at about 3400 cm^{-1} , to the hydroxyl band. The infrared spectrum of the material treated with borane complex (trace B) shows the reduction of the carboxyl groups from MWCNT-COOH to hydroxymethyl (MWCNT-CH₂OH) as indicated by the disappearance of the C=O bands and the appearance of two small peaks at ~ 2900 and 2850 cm^{-1} corresponding to the C-H stretching vibrations of the methylene group. The infrared spectrum for MWCNT-CH₂OTs contains bands characteristic of tosylate esters at approximately 1190 , 1380 , and 660 cm^{-1} . The FTIR spectrum of the MWCNT-Phen-ether presents several characteristic bands: C-O-C stretch at about 1120 and 1300 cm^{-1} ;

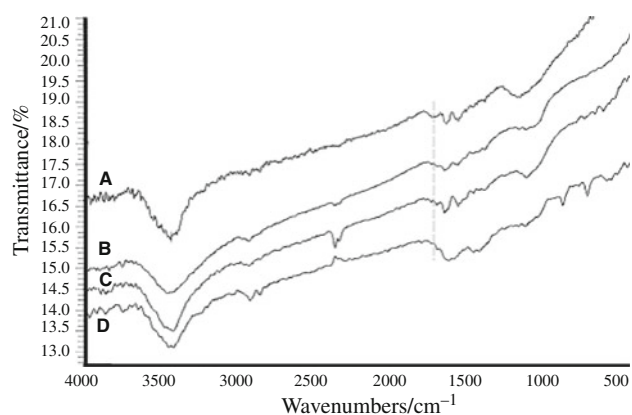
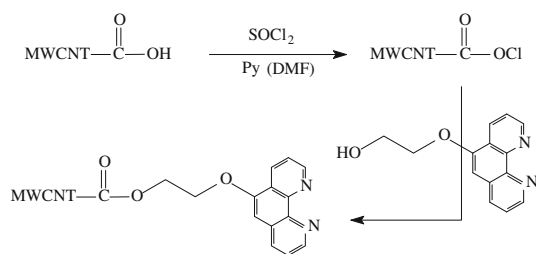


Fig. 4 Infrared spectra of functionalized MWCNT-carboxyl through ether-linked phenanthroline. MWCNT-COOH (A), MWCNT-CH₂OH (B), MWCNT-CH₂OTs (C), MWCNT-Phen-ether (D)



Scheme 3 Attachment of a 1,10-phenanthroline unit to MWCNT via an ester linkage

aromatic nucleus at ~ 1600 and 1475 ; and C-N stretch (aryl) at 1360 cm^{-1} . Also C-H (aromatic) bands are present at about 690 and 880 cm^{-1} (bend) and 3020 cm^{-1} (stretch).

In a second approach (Scheme 3), carboxyl groups at the surface of the nanotubes were converted to the corresponding acid chloride and treated with 5-(2-hydroxyethoxy)-1,10-phenanthroline to attach the phenanthroline ligand via an ester linkage.

This adduct was also characterized using infrared spectroscopy (see Fig. 5).

In the ester-linked phenanthroline-MWCNT (MWCNT-Phen-ester) the most interesting band is that found at about 1735 cm^{-1} (as compared to 1720 cm^{-1} in MWCNT-COOH (A) and 1710 cm^{-1} in MWCNT-COCl (B) indicating that phenanthroline ligand was covalently bound to the MWCNT through an ester linkage.

The thermal decomposition of these derivatives was also examined using thermogravimetry. Thermograms for the decomposition of the carboxyl-functionalized MWCNT, the corresponding acid chloride and the ester-bound 1,10-phenanthroline are displayed in Fig. 6.

The thermogram for the decomposition (in air) of the ester precursor is included for comparison. The thermal degradation of the ester-bound-1,10-phenanthroline-MWCNT is

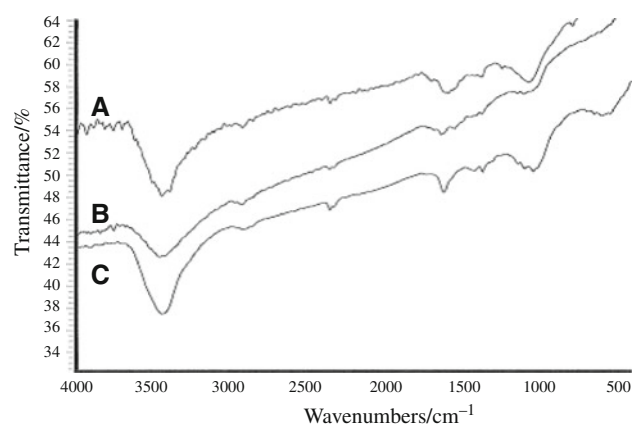


Fig. 5 Infrared spectra of carboxyl-functionalized MWCNT (MWCNT-COOH, A), the corresponding acid chloride (MWCNT-COCl, B), and ester-linked phenanthroline-MWCNT (MWCNT-Phen-ester, C)

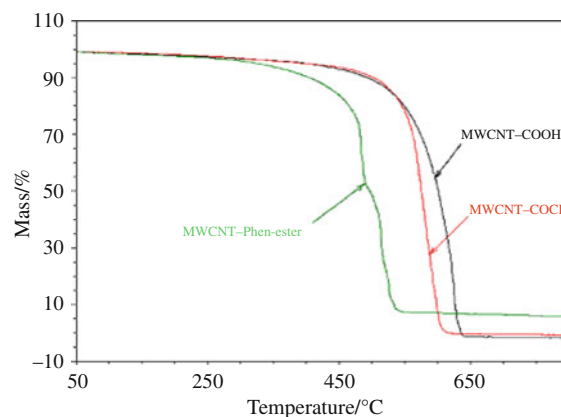


Fig. 6 Thermal degradation in an air atmosphere of functionalized MWCNT-carboxyl through ester-linked phenanthroline

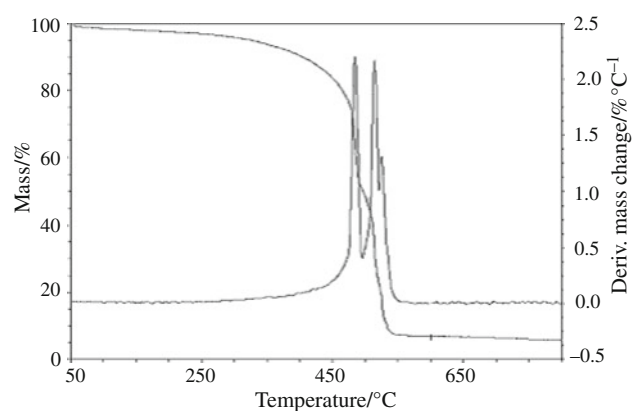


Fig. 7 Thermal degradation in an air atmosphere of MWCNT containing ester-linked phenanthroline at the surface

depicted in Fig. 7. Decomposition occurs smoothly in three stages. The first occurs at an extrapolated onset temperature of 477 °C and reflects fragmentation of the attached ligand.

Conclusions

A good complexing ligand, 1,10-phenanthroline, may be tethered to MWCNT by either ether or ester linkages. The thermal stability of these adducts as determined by thermogravimetry is sufficient to permit their use in a variety of applications including robust heterogeneous catalyst systems that may be recycled repeatedly. While the ether-linked adduct will likely be the most durable (less sensitive to hydrolysis, etc.), both adducts display good thermal stability with extrapolated onset temperature for degradation of >400 °C. The mode of degradation is different for the two adducts. The ether-linked adduct apparently undergoes degradation via scission of the attachment to the MWCNT while the ester-linked adduct degradation reflects decomposition of the ligand.

References

1. Iijima S. Helical microtubules of graphitic carbon. *Nature*. 1991;354(6348):56–8.
2. Meyyappan M, editor. Carbon nanotubes: science and applications. Boca Raton: CRC Press; 2005.
3. O'Connell MJ, editor. Carbon nanotubes: properties and applications. Boca Raton: CRC Press; 2006.
4. Peng X, Wong SS. Functional covalent chemistry of carbon nanotube surfaces. *Adv Mater*. 2009;1(6):625–42.
5. Cao Q, Rogers JA. Ultrathin films of single-walled carbon nanotubes for electronics and sensors: a review of fundamental and applied aspects. *Adv Mater*. 2009;21(1):29–53.
6. Merkoci A. Carbon nanotubes in analytical sciences. *Microchim Acta* 2006;152:157–174.
7. Katok KV, Tertykh VA, Brichka SYa, Prikho'ko GP. Catalytic synthesis of carbon nanotubes ordered mesoporous matrices. *J Therm Anal Calorim*. 2006;86(1):109–14.
8. Marshall MW, Popa-Nita S, Shapter JG. Measurement of functionalized carbon nanotube carboxylic acid groups using a simple chemical process. *Carbon*. 2006;44(7):1137–41.
9. Blanchnio M, Staszczuk P, Grodzicka G. Adsorption and porosity properties of pure and modified carbon nanotubes surfaces. *J Therm Anal Calorim*. 2008;94(3):641–8.
10. Hu H, Bhowmik P, Zhao B, Harmon MA, Hkis ME, Haddon RC. Determination of the acidic sites of purified single-walled carbon nanotubes by acid-base titration. *Chem Phys Lett*. 2001;345(1–2):25–8.
11. Mawhinney DB, Naumenko V, Kuznetsova A, Yates JT, Liu J, Smalley RE. Surface defect site density on single walled carbon nanotubes by titration. *Chem Phys Lett*. 2000;324(1–3):213–6.
12. Hamon MA, Hu H, Bhowmik P, Niyogi S, Zhao B, Htkis ME. End-group and defect analysis of soluble single-walled carbon nanotubes. *Chem Phys Lett*. 2001;347(1–3):8–12.
13. Lee HJ, Oh S-J, Cho J-Y, Kim JW, Tan L-S, Back JB. In situ synthesis of poly(ethylene terephthalate) (PET) in ethylene glycol containing terephthalic acid and functionalized multiwalled carbon nanotubes (MWNTs) as an approach to MWNT/PET nanocomposites. *Chem Mater* 2005;17(20):5057–5064 (and references edited therein).
14. Liu P. Modifications of carbon nanotubes with polymers. *Eur Polym J*. 2005;41(11):2693–703.
15. Chen G-X, Kim H-S, Park BH, Yoon J-S. Controlled functionalization of multiwalled carbon nanotubes with various molecular-mass poly(L-lactic acid). *J Phys Chem B*. 2005;109(47):22237–43.
16. Qin S, Qin D, Ford WT, Resasco DE, Herrera JE. Functionalization of single-walled carbon nanotubes with polystyrene via grafting to and grafting from methods. *Macromolecules*. 2004;37(3):752–7.
17. Qin S, Qin D, Ford WT, Zhang Y, Kotov NA. Covalent cross-linked polymer/single-wall carbon nanotube multilayer films. *Chem Mater*. 2005;17:2131–5.
18. Homenick CM, Sivasubrameniam U, Adronov A. Effect of polymer chain length on the solubility of polystyrene grafted single-walled carbon nanotubes in tetrahydrofuran. *Polym Int*. 2008;57(8):1007–11.
19. Mansky P, Liu Y, Huang E, Russell TP, Hawker CJ. Controlling polymer-surface interactions with random copolymer brushes. *Science*. 1997;275(5305):1458–60.
20. Cao L, Yang W, Yang J, Wong C, Fu S. Hyperbranched poly(amidoamine)-modified multi-walled carbon nanotubes via grafting-from method. *Chem Lett*. 2004;33(5):490–1.
21. Priftis D, Sakellariou G, Hadjichristidis N, Penott EK, Lorenzo AT, Muller AJ. Surface modification of multiwalled carbon nanotubes with biocompatible polymers *via* ring opening and living anionic surface initiated polymerization. Kinetics and crystallization behavior. *J Polym Sci Polym Chem*. 2009;47(17):4379–90.
22. Yao Z, Braidy N, Bolton GA, Adronov A. Polymerization from the surface of single-walled carbon nanotubes—preparation and characterization of nanocomposites. *J Am Chem Soc*. 2003;125(51):16015–24.
23. Kong H, Gao C, Yan D. Controlled functionalization of multiwalled carbon nanotubes by in situ atom transfer radical polymerization. *J Am Chem Soc*. 2004;126(2):412–3.
24. Kong H, Luo P, Gao C, Yan D. Polyelectrolyte-functionalized multiwalled carbon nanotubes: preparation, characterization and layer-by-layer self-assembly. *Polymer*. 2005;46(8):2472–85.
25. Kotal A, Mandal TK, Walt DR. Synthesis of gold-poly(methyl methacrylate) core-shell nanoparticles by surface-confined atom transfer radical polymerization at elevated temperature. *J Polym Sci Polym Chem*. 2005;43(16):631–42.
26. Pei X, Hao J, Liu W. Preparation and characterization of carbon nanotubes-polymer/Ag hybrid nanocomposites via surface RAFT polymerization. *J Phys Chem C*. 2007;111(7):2947–52.
27. You Y-Z, Hong C-Y, Pan C-Y. Preparation of smart polymer/carbon nanotube conjugates *via* stimuli-responsive linkages. *Adv Funct Mater*. 2007;17(14):2470–7.
28. Zhao X, Lin W, Song N, Chen X, Fan X, Zhou Q. Water soluble multi-walled carbon nanotubes prepared *via* nitroxide-mediated radical polymerization. *J Mater Chem*. 2006;16(47):4619–25.
29. Lu F, Gu L, Meziani MJ, Wang X, Luo PG, Veca LM, et al. Advances in bioapplications of carbon nanotubes. *Adv Mater*. 2009;21(2):139–52.
30. Kim T-W, Chung P-W, Slowing II, Tsunoda M, Yeung ES, Liu VS-Y. Structurally ordered mesoporous carbon nanoparticles as transmembrane delivery vehicle in human cancer cells. *Nano Lett*. 2008;8(11):3724–7.
31. Prato M, Kostarelos K, Bianco A. Functionalized carbon nanotubes in drug design and discovery. *Acc Chem Res*. 2008;41(1):60–8.
32. Liu Z, Winters M, Holodny M, Dai HJ. siRNA delivery into human T cells and primary cells with carbon-nanotube transporters. *Angew Chem Int Ed*. 2007;46(12):2023–7.
33. Liu Z, Cai W, He L, Nakayama N, Sun X, Chen X, et al. In vivo biodistribution and highly efficient tumour targeting of carbon nanotubes in mice. *Nat Nanotechnol*. 2007;2(1):47–52.

34. Dhar S, Liu Z, Thomale J, Dai H, Lippard SJ. Targeted single-wall carbon nanotube-mediated Pt(IV) prodrug delivery using folate as a homing device. *J Am Chem Soc.* 2008;130(34):11467–76.
35. Feazell RP, Nakayama-Ratchford N, Dai H, Lippard SJ. Soluble single-walled carbon nanotubes as longboat delivery systems for platinum(IV) anticancer drug design. *J Am Chem Soc.* 2007;129(27):8349–438.
36. Howell BA, Fan D, Rakesh L. Nanoscale dendrimer-platinum conjugates as multivalent antitumor drugs. In: Abd-El-Aziz AS, Carraher CE, Pittman CU, Zeldin M, editors. *Inorganic and organometallic macromolecules: design and applications.* New York: Springer Science; 2008. p. 269–94.
37. Antkowiak R, Antkowiak W. Chlorine addition to the C(5)-C(6) bridge and N-oxidation of 1,10-phenanthroline. *Heterocycles.* 1998;47(2):893–909.
38. Krishnan S, Kuhn DJ, Hamilton GA. Direct oxidation in high yield of some polycyclic aromatic compounds to arene oxides using hypochlorite and phase transfer catalysts. *J Am Chem Soc.* 1997;99(24):8121–3.
39. Shen Y, Sullivan BP. A versatile preparative route to 5-substituted-1,10-phenanthroline ligands via 1,10-phenanthroline 5,6-epoxide. *Inorg Chem.* 1995;34(25):6235–6.
40. Slough GA, Krehnak V, Helquist P, Canham SM. Synthesis of readily cleavable immobilized 1,10-phenanthroline resins. *Org Lett.* 2004;6(17):2909–12.
41. Paris J, Gameiro C, Humblet V, Mohapatra PK, Jacques V, Desreux JF. Auto-assembling of ditopic macrocyclic lanthanide chelates with transition-metal ions. Rigid multimetallic high relaxivity contrast agents for magnetic resonance imaging. *Inorg Chem.* 2006;45(13):5092–102.
42. Zacharias DE, Case FH. Substituted 1,10-phenanthrolines. XIV. Hydroxy and methoxy derivatives. *J Org Chem.* 1962;27:3878–82.
43. Gruijters BWT, Broeren MAC, van Delft FL, Sijbesma RP, Hermkens PHH, Rutjes FPJT. Catalyst recycling via hydrogen-bonding-based affinity tags. *Org Lett.* 2006;8(15):3163–6.
44. Bolton KF, Canty AJ, Deverell JA, Guijit RM, Hilder EF, Rodemann T, et al. Macroporous monolith supports for continuous flow capillary microreactors. *Tetrahedron Lett.* 2006;47(52):9321–4.
45. Yoon NM, Pak CS, Brown HC, Krishnamurthy S, Stokly TP. Selective reductions. XIX. Rapid reaction of carboxylic acids with borane-tetrahydrofuran. Remarkably convenient procedure for the selective conversion of carboxylic acids to the corresponding alcohols in the presence of other functional groups. *J Org Chem.* 1973;38(16):2786–92.
46. Jockel H, Schmidt RJ. Kinetics of the borane reduction of pinacolone in THF catalyzed by two different oxazaboroles. *J Chem Soc Perkin Trans* 1997;2(12):2719–2723.
47. Tipson RS. Esters of *p*-toluenesulfonic acid. *Org Chem.* 1944;9:235–41.
48. Koch JK, Hammond GS. Benzyl tosylates. I. Preparation and properties. *J Am Chem Soc.* 1953;75:3443–4.
49. Accorsi G, Listorti A, Yoosaf K, Armaroli N. 1,10-Phenanthrolines: versatile building blocks for luminescent molecules, materials and metal complexes. *Chem Soc Rev.* 2009;38(6):1690–700.
50. Sammes PG, Yahioighu G. 1,10-Phenanthroline: a versatile ligand. *Chem Soc Rev.* 1994;23(5):327–34.
51. Williams JAG. Photochemistry and photophysics of coordination compounds: Platinum. *Top Curr Chem.* 2007;281:205–68.